Complete determination of the state of elliptically polarized light by electron-ion vector correlations

K. Veyrinas,* C. Elkharrat, S. Marggi Poullain, N. Saquet, and D. Dowek,†
Institut des Sciences Moléculaires d'Orsay (UMR 8214 CNRS-Université Paris Sud), Bâtiment 350, Université Paris Sud, 91405 Orsay Cedex, France

R. R. Lucchese
Department of Chemistry, Texas A&M University, College Station, Texas 77843, USA

G. A. Garcia and L. Nahon
Synchrotron SOLEIL, L'Orme des Merisiers, St. Aubin BP 48, 91192 Gif sur Yvette, France
(Received 1 August 2013; published 20 December 2013)

We propose a method, molecular polarimetry, applicable to an extended VUV–x-ray range, allowing us to determine the complete state of elliptically polarized light, including the challenging disentanglement of the circular and unpolarized components. It relies on the determination of the molecular frame photoelectron angular distributions derived from electron-ion velocity vector correlations in dissociative photoionization of simple molecules. The high accuracy of the full set of Stokes parameters determination has been established by comparison with data obtained in parallel with a VUV optical polarimeter used as a benchmark.

DOI: 10.1103/PhysRevA.88.063411 PACS number(s): 33.80.Eh, 33.55.+b, 07.60.Fs

I. INTRODUCTION

As a vectorial property of light, polarization is able to reveal fundamental geometrical and symmetry properties of matter. Circularly polarized light (CPL) defines a three-dimensional (3D) orientation in space so that it is sensitive to both intrinsic molecular chirality [1,2] and extrinsic chirality where the handedness is achieved by the combined system of photon and molecule [3–5]. The latter is illustrated, e.g., by the circular dichroism in the angular distribution (CDAD), which measures the variation of the molecular frame photoelectron angular distributions (MFPADs) of an achiral molecule when exposed to left- or right-handed CPL [6–11]. Reciprocally, matter may probe the polarization of incident light. The simplest example is that of PADs of atoms in photoionization (PI) induced by linearly polarized light which presents an anisotropy, encapsulated in the asymmetry parameter β_e, whose intensity scales with the degree of polarization ([12] and references therein). This was confirmed by Takahashi *et al.* [13], who probed the linearly polarized components of light, by measuring the PADs using a velocity imaging analyzer in the PI of He, and provided a direct comparison with an optical method based on a single rotating multilayer polarizer.

With the unprecedented performance of novel VUV and x-ray sources, such as high harmonic generation (HHG), free-electron lasers (FELs), or third generation synchrotron radiation (SR), more experiments relying on light-matter interaction call for an accurate knowledge of the polarization state of the incident or emitted light in order to understand and normalize CD data [14], as well as to optimize the production of CPL and unravel possible distortions due to the light generation process itself or to the optics used to shape the beam [15,16].

There is therefore a crucial need for *in situ* polarimetry providing an accurate full polarization ellipse determination. This is usually achieved by optical methods using sophisticated *in vacuo* polarimeters based upon reflections on mirrors in the VUV range [17] or reflections and transmission on multilayers in soft–x-ray range dedicated ellipsometers [18], providing the normalized Stokes parameters (s_1, s_2, s_3) which characterize the linear (s_1, s_2) and circular (s_3) polarized intensities [19]. However, such polarimeters operate in general only at a few selected wavelengths [20], so that their use appears limited especially as realization and characterization [21] of optics in such ranges are very challenging. Another method consists of transforming short-wavelength radiation into UV-visible radiation using, e.g., resonance absorption in the VUV range and subsequent fluorescence [22,23].

Several alternative polarimetry techniques are based upon the measurement of the intensity of various types of CD on a reference sample. This is for instance the case of x-ray magnetic CD (XMCD) which can provide quite accurate values of s_3, and only s_3, [24] at a few selected photon energies in the soft–x-ray range corresponding to absorption edges of the considered material.

Nonoptical methods aiming at the determination of the full polarization ellipse, and especially the challenging disentanglement of the circular and unpolarized components, require to set a handedness in the probe system and to measure a CD effect. In one-photon PI of atoms or achiral molecules, it is achievable if three noncoplanar vectors can be defined. In the pioneering scheme of Lörch *et al.* [25] addressing PI of atoms, an angle-resolved photoelectron–Auger-electron coincidence setup allowed them to extract all Stokes parameters for partially polarized soft–x-ray light. This method, restricted to inner-shell ionization involving Auger decay, requires a precise knowledge of the PI matrix elements including their relative phases. A recent theoretical study predicting a CD in photoelectron spectra structured by the sidebands in IR laser-assisted XUV short-pulse PI of atoms [26], also pointed out that this effect could be used for measuring circular polarization of x rays.

*kevin.veyrinas@u-psud.fr
†danielle.dowek@u-psud.fr

In this paper, we present an original molecular polarimetry (MP) method relying on dissociative photoionization (DPI) of simple molecules valid over the whole range from VUV to x-ray wavelengths [27,28]. It is based upon the analysis of the ($\mathbf{V_{i+}}$, $\mathbf{V_e}$, $\mathbf{k}$) noncoplanar vector correlation, where $\mathbf{V_{i+}}$ and $\mathbf{V_e}$ are the coincident electron-ion velocity vectors and $\mathbf{k}$ is the light propagation axis. By comparison with data obtained in parallel using an *in situ* insertable VUV optical polarimeter [29], we show that indeed a molecule is able to accurately disclose the full polarization ellipse and absolute rate of polarization of an incoming photon, even in the case of a general elliptical polarization.

II. EXPERIMENTAL METHOD

The polarization state of the light is described by the four normalized Stokes parameters (s_1,s_2,s_3,s_4) [19]. $\sqrt{s_1^2+s_2^2+s_3^2}$ and $s_4 = 1-\sqrt{s_1^2+s_2^2+s_3^2}$ represent the intensity of the polarized and unpolarized components respectively.

Experiments were performed on the DESIRS VUV beamline at SOLEIL [30], equipped with a variable polarization undulator able to produce any tailored polarization ellipse, and using the vector correlation (VC) method [31], which consists of measuring in coincidence the emission velocity vectors of the ion fragment and the photoelectron resulting from each single DPI event. Briefly, the interaction region located at the center of the VC double velocity spectrometer [32,33] is defined by the intersection between a supersonic molecular beam and the elliptically polarized SR ($\mathbf{k}$ propagation vector along the y axis; see Fig. 1).

Ions and electrons are guided to their respective time and position sensitive detectors by a dc electric field $\mathbf{E}$ coupled to a set of focusing electrostatic lenses, such that a 4π collection of both particles is ensured. The $\mathbf{V_{i+}}$ ion fragment and $\mathbf{V_e}$ electron vectors are derived from their impact positions and time of flights. Note that this 3D electron-ion imaging requires that the SR is operated in the temporal structure mode of SOLEIL (147-ns period, 50-ps pulse width), although more limited information is obtained using the quasi-cw multibunch mode as discussed below.

Just upstream from the VC setup, with no optics in between, sits the insertable *in situ* VUV optical polarimeter [29]. It is based upon two co-axially rotating elements, acting respectively as a dephazer and an analyzer by reflexions on a prism and a flat mirror. The measurement of the modulated transmitted flux as a function of the two azimuthal angles of the rotating elements provides the four Stokes parameters without any prior knowledge of the optical properties of the polarimeter. The optical polarimetry (OP) measurements were made, *in vacuo*, just before the VC measurements, which were carried out by simply removing the prisms from the beam.

III. RESULTS

We demonstrate the MP method by studying the benchmark DPI reaction of the NO molecule induced at a photon excitation energy of $h\nu = 23.65$ eV:

$$\begin{aligned} \mathrm{NO}(X\,^2\Pi) + h\nu(\hat{\mathbf{e}}) &\rightarrow \mathrm{NO}^+(c\,^3\Pi) + e \\ &\rightarrow \mathrm{N}^+(^3P) + O(^3P) + e, \end{aligned} \qquad (1)$$

leading to ion fragment and photoelectron kinetic energies of ~0.4 eV and ~1.9 eV respectively [31,33]. This process was chosen because (i) the dominant parallel character ($\Delta\Lambda = 0$) of the electric dipole transition (1) results in a significant N^+ emission anisotropy characterized by an asymmetry parameter $\beta_{N+} \approx 1$ [31]; (ii) the CDAD is significant [10]. The (N^+,e) coincident events attributed to reaction (1) are selected using the electron-ion kinetic-energy correlation diagram (KECD) derived from the scalar analysis of the ($\mathbf{V_{N+}}$, $\mathbf{V_e}$, $\mathbf{k}$) vector correlation [31]. Figure 2(a) displays three 2D histograms of these events as a function of the V_{xi} and V_{zi} components of the N^+ velocity in the polarization plane perpendicular to the propagation axis $\mathbf{k}$, obtained for

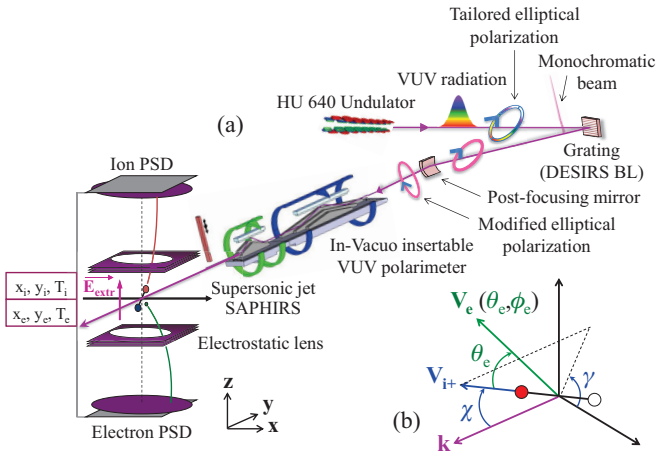

FIG. 1. (Color online) Scheme of the experimental setup including the optical VUV polarimeter and the VC spectrometer acting as molecular polarimeter (a). Sketch of the $V_{i+}(\chi,\gamma)$ and $V_e(\theta_e,\phi_e)$ velocity vectors and emission angles in the laboratory (ion) and molecular frame (electron), respectively (b).

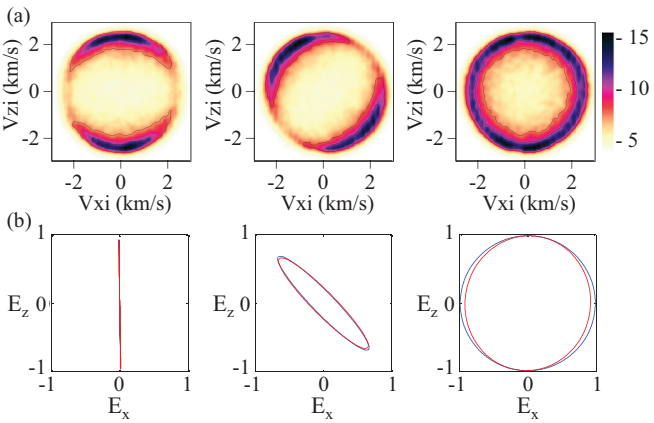

FIG. 2. (Color online) (V_{xi}, V_{zi}) 2D histograms of the (N^+,e) events for reaction (1) for three selected polarization states of the light (see text) (a) and corresponding (E_x, E_z) normalized polarization ellipses retrieved by optical (OP: blue) and molecular (MP: red) polarimetry (b).

three selected polarization states of the incident light. They reveal unambiguously the direction of the main axis of the polarization ellipse along the z axis, tilted at 45° relative to the z axis, or the circular (or totally unpolarized) character of the polarization.

Beyond this first qualitative evidence of polarization properties, the determination of the Stokes parameters relies on the analysis of the $I(\theta_e, \phi_e, \chi, \gamma)$ MFPAD whose general expression for ionizing elliptically polarized light is written as [10,28]:

$$
\begin{aligned}
I(\theta_e,\phi_e,\chi,\gamma) = {} & F_{00}(\theta_e) + F_{20}(\theta_e)\left[-\frac{1}{2}P_2^0(\cos\chi) + t_1(\gamma)Q_0^+(\chi)\right] \\
& + F_{21}(\theta_e)\left\{\left[-\frac{1}{2}P_2^1(\cos\chi) + t_1(\gamma)Q_1^+(\chi)\right]\cos(\phi_e) + t_2(\gamma)Q_1^-(\chi)\sin(\phi_e)\right\} \\
& + F_{22}(\theta_e)\left\{\left[-\frac{1}{2}P_2^2(\cos\chi) + t_1(\gamma)Q_2^+(\chi)\right]\cos(2\phi_e) + t_2(\gamma)Q_2^-(\chi)\sin(2\phi_e)\right\} - s_3 F_{11}(\theta_e)P_1^1(\cos\chi)\sin(\phi_e)
\end{aligned}
$$

$$
\begin{aligned}
\text{with} \quad & t_1(\gamma) = s_1\cos(2\gamma) - s_2\sin(2\gamma) \\
& t_2(\gamma) = s_1\sin(2\gamma) + s_2\cos(2\gamma) \quad \text{and} \\
& Q_N^{\pm}(\chi) = \frac{3}{(2-N)!}\{(-1)^N[\cos(\chi/2)]^{2+N}[\sin(\chi/2)]^{2-N} \pm [\cos(\chi/2)]^{2-N}[\sin(\chi/2)]^{2+N}\}. \qquad (2)
\end{aligned}
$$

Here the angles (θ_e, ϕ_e) and (χ, γ) define the emission direction of the photoelectron in the molecular frame and of the ion in the laboratory frame, respectively, as sketched in Fig. 1. The five one-dimensional $F_{\mathrm{LN}}(\theta_e)$ functions are expressed in terms of the dipole matrix elements of the PI reaction [10], and P_L^N are the Legendre polynomials.

The evaluation of the Stokes parameters proceeds in two steps. First, after summing over the photoelectron emission angles, the $I(\theta_e, \phi_e, \chi, \gamma)$ angular distribution (2) reduces into the $I(\chi, \gamma)$ ion fragment angular distribution in the laboratory frame given in Eq. (3):

$$
I(\chi,\gamma) = C\left(1 + \beta_{N^+}\left[-\frac{1}{2}P_2^0(\cos\chi) + \frac{1}{4}t_1(\gamma)P_2^2(\cos\chi)\right]\right). \qquad (3)
$$

Such 2D histograms are displayed in Fig. 3 for the three polarizations involved in Fig. 2(a). The Fourier analysis of the two projections of this histogram enables us to determine the s_1 and s_2 Stokes parameters and the corresponding statistical error bars, provided that the β_{N+} asymmetry parameter also determined in the analysis is nonzero.

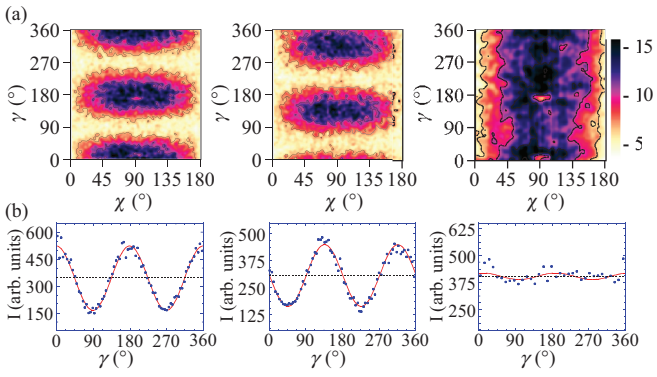

FIG. 3. (Color online) $I(\chi, \gamma)$ histograms of the events for the three polarization states of the light described in the text (a) and corresponding $I(\gamma)$ N^+ ion fragment azimuthal angle distributions, corresponding to the projection of the $I(\chi, \gamma)$ distributions onto the vertical axis; the phase shifts observed in the azimuthal dependence of the intensity distribution reflect different sets of s_1 and s_2 Stokes parameters (b).

If we now progress in the analysis of Eq. (2) we note that, ignoring the γ ion fragment azimuthal dependence, the $I(\theta_e, \phi_e, \chi)$ distribution is formally identical to the general form of the MFPAD for PI of a linear molecule induced by circularly polarized light [10,34], except for the circular dichroism term F_{11} which is here multiplied by the Stokes parameter s_3. Therefore, the product $s_3 \cdot F_{11}$ is the measured mixed quantity and the determination of the s_3 Stokes parameter relative to the circularly polarized part of the light requires the knowledge of the F_{11} function for the studied process, from an independent experiment or calculation. For simplicity we choose here to present the results in terms of the dimensionless $\mathrm{CDAD}(\theta_e)$ function (4), proportional to F_{11}, which characterizes the MF photoemission in the polarization half plane ($\phi_e = 90°$) when the molecular axis is perpendicular to the light propagation axis ($\chi = 90°$). In this plane, it is defined as the relative variation of the $I(\theta_e, \phi_e = 90°, \chi = 90°)$ MFPAD when the helicity h of the light is changed from $+1$ (left-handed CPL) to -1 (right-handed CPL) [35]:

$$
\begin{aligned}
\mathrm{CDAD}(\theta_e) &= \frac{I_{+1} - I_{-1}}{I_{+1} + I_{-1}} \\
&= \frac{2F_{11}(\theta_e)}{2F_{00}(\theta_e) + \frac{1}{2}F_{20}(\theta_e) + 3F_{22}(\theta_e)}. \qquad (4)
\end{aligned}
$$

$\mathrm{CDAD}(\theta_e)$ can also be obtained from the left-right emission asymmetry in the polarization plane ($\phi_e = 90°$ or 270°), $\frac{I_{90} - I_{270}}{I_{90} + I_{270}}$, for a pure CPL ($h = +1$). In the case of an elliptically polarized light characterized by a s_3 Stokes parameter, this quantity is equal to $-s_3 \cdot \mathrm{CDAD}(\theta_e)$. Figure 4 displays a comparison between the CDAD measured in an experiment performed with pure left-handed CPL ($s_3 = -1$, used as a reference), the product $-s_3 \cdot \mathrm{CDAD}$ corresponding to the unknown polarization named "Elliptic 1" in Table I and computed CDAD based on multichannel Schwinger configuration

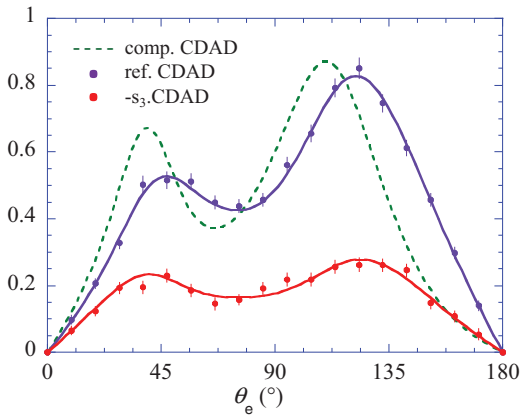

FIG. 4. (Color online) Measured reference CDAD for reaction (1) using pure left-handed CPL with $s_3 = -1$ (violet dots), $-s_3$·CDAD measured for the "Elliptic 1" polarization in Table I (red dots), and MCSCI computed CDAD convoluted with the apparatus function (green dashed line). The violet and red lines are derived from a Legendre polynomial fit of the measured F_{LN} functions [36] which also provides the statistical error bars.

interaction calculations [10], convoluted with the apparatus function. The value of the unknown s_3 parameter, here $s_3 \approx -0.36$, is readily deduced by fitting the measured $-s_3$·CDAD by the reference CDAD. Although experiment and theory are in quite good qualitative agreement, we note that using the calculation as a reference here would not provide such a precise determination of s_3.

Table I displays the Stokes parameters measured using the MP and the optical methods, with the s_4 component is given by $s_4 = 1 - \sqrt{s_1^2 + s_2^2 + s_3^2}$. The corresponding polarization ellipses for various polarization states of the incoming light are displayed in Fig. 2(b). Both expressions of the results show that the outcome of the MP method is in very good agreement, especially regarding the s_3 parameter, with the results obtained using the *in situ* VUV optical polarimeter, even in the case of a small intentionally produced unpolarized contribution (Elliptic 2).

We estimate the absolute error bars of the optical polarimetry method to be as low as 0.01, as deduced from the quality of the least-squares fit to the data, including the dispersion on the photon signal measurements and systematic errors which would deviate experimental points from the ideal behavior such as co-axiality of the rotating motions of the polarimeter [29] and error bars on the polarimeter optical constants. Such error bars appear to be realistic considering the high s_1 values of ± 0.99 as measured in the most trivial cases of pure linear polarization (horizontal and vertical) very close to the expected ± 0.99 to ± 1.00 values [30]. As for the molecular polarimetry method, the precision in the determination of the Stokes parameters results from two components due to statistical and systematic errors, the latter being defined as the influence of the apparatus function onto the measured F_{LN} functions and CDAD. Typical statistical error bars for the data reported in Table I, each measurement corresponding to the acquisition of about 10^5 (N^+,e) events for the studied process in 40 min, are of the order of 0.02. The comparison of the Stokes parameters MP values with those obtained by the optical method indicates that systematic errors must be negligible in present conditions. More generally, minimizing systematic errors in the design of a specific instrument for polarimetry metrological purposes can be optimized based on Monte Carlo simulation of the particle trajectories for a given geometry of the spectrometer, taking into account the characteristics of the interaction region and the temporal and spatial resolutions of the detection system.

At other photon energies in the VUV range, the method is readily applicable if one selects a target molecule for which DPI is an opened channel, producing photoelectron of kinetic energy in the 0–15-eV range allowing for a complete MFPAD determination. This energy maximal value depends on the scheme of the spectrometer, and would be larger if one uses, e.g., detectors of larger diameter, or a COLTRIMS setup: this is to be considered when building up a prototype dedicated instrument. In the x-ray regime where inner-shell ionization occurs, DPI strongly dominates so that the only issue is to select a target which contains atoms with inner-shell photoionization thresholds leading to the production of several eV photoelectrons [27].

Finally, it is worth discussing the outcome of the MP method when the synchrotron is run in the "multibunch mode" which precludes measuring the photoelectron V_{ze} component. This causes a loss in electron energy resolution and prevents the access to the complete MFPAD. Based on the achieved information for each coincident DPI event, consisting of the five (V_{xi}, V_{yi}, V_{zi}, V_{xe}, V_{ye}) quantities, one can still operate a relevant selection of processes satisfying the condition of a nonzero ion fragment asymmetry parameter. The corresponding $I(\chi, \gamma)$ histogram enables extraction of the s_1 and s_2 Stokes parameters. Note that ion fragment 3D momentum imaging which provides the $I(\chi, \gamma)$ histogram can also be achieved in noncoincidence experiments, i.e., ignoring the electron detection. The magnitude of the s_3 parameter, in such restricted conditions, can then be obtained when the light is fully polarized, i.e., $s_4 = 0$.

TABLE I. Stokes parameters determined by (left) molecular polarimetry and (right) the VUV optical polarimeter. Multi-B refers to a measurement recorded using the "multibunch mode": in this case the magnitude of s_3 can be deduced from s_1 and s_2, assuming that s_4 is equal to 0 (see text).

	s_1	s_2	s_3	s_4	s_1	s_2	s_3	s_4
Vertical	−0.97	−0.03	0.00	0.03	−0.97	−0.02	0.00	0.03
Pure CPL	−0.07	0.02	−0.99	0.01	0.00	0.07	−0.99	0.01
Elliptic 1	−0.02	−0.90	−0.36	0.03	−0.04	−0.90	−0.35	0.04
Elliptic 2	−0.01	−0.86	−0.32	0.08	−0.03	−0.90	−0.30	0.05
Multi-B	0.06	0.94	±0.33		0.14	0.94	−0.32	0

IV. CONCLUSION

In conclusion, we have reported and validated, by comparing with data obtained with an optical polarimeter used as a benchmark, an original MP method based on the analysis of MF photoemission in a DPI reaction, which encapsulates the full polarization state of the incoming photon. Indeed, both methods give access to the relative phase of the incoming light components either with the dephazer optical element, or via the determination of the F_{11}/CDAD dynamical parameters and comparison with a pure CPL reference in MP. This approach possesses three very attractive features: Giving access to the full polarization ellipse allows the complete disentanglement of s_3 and s_4. Second, since an increasing number of imaging devices are equipping end stations of SR or HHG and FELs short-wavelength sources, it becomes more accessible and easier to implement. Finally, this method is completely tunable and universal since it can be applied to any wavelength range, selecting adequately relevant ionization thresholds. Several applications of the MP method are foreseen, such as setting up dedicated apparatus to characterize VUV and x-ray sources (SR, FELs, and HHG) and control the stability of their polarization properties [16], or address physical issues where the light polarization state is a fingerprint of, e.g., symmetry breaking in the generating medium [15].

ACKNOWLEDGMENTS

We are grateful to the SOLEIL general staff for running smoothly the facility and to J. F. Gil for technical help on the beamline. We gratefully acknowledge the contribution of M. Lebech, P. Billaud, and Y. J. Picard to experiments, S. Lupone for technical support, and J. C. Houver for the development of data analysis software. R.R.L. acknowledges the support of the Office of Basic Energy Sciences, US Department of Energy, and of the Robert A. Welch Foundation (Houston, TX) under Grant No. A-1020. The support of the PICS (Programme International de Coopération Scientifique CNRS No. 2008-046T) and the Triangle de la Physique (MOF-MPI No. 2013-0569T) is gratefully acknowledged.

[1] L. D. Barron, *Molecular Light Scattering and Optical Activity* (Cambridge University Press, Cambridge, England, 2004).
[2] N. Berova, K. Nakanishi, and R. Woody, *Circular Dichroism: Principles and Applications* (Wiley-VCH, New York, 2000).
[3] R. L. Dubs, S. N. Dixit, and V. McKoy, Phys. Rev. Lett. **54**, 1249 (1985).
[4] N. A. Cherepkov, Chem. Phys. Lett. **87**, 344 (1982); N. A. Cherepkov and V. V. Kuznetsov, Z. Phys. D **7**, 271 (1987).
[5] G. Schönhense, Phys. Scr. **T31**, 255 (1990).
[6] K. L. Reid, Mol. Phys. **110**, 131 (2012).
[7] S. Motoki, J. Adachi, K. Ito, K. Ishii, K. Soejima, A. Yagishita, S. K. Semenov, and N. A. Cherepkov, Phys. Rev. Lett. **88**, 063003 (2002).
[8] T. Jahnke *et al.*, Phys. Rev. Lett. **88**, 073002 (2002).
[9] O. Gessner, Y. Hikosaka, B. Zimmermann, A. Hempelmann, R. R. Lucchese, J. H. D. Eland, P. M. Guyon, and U. Becker, Phys. Rev. Lett. **88**, 193002 (2002).
[10] M. Lebech *et al.*, J. Chem. Phys. **118**, 9653 (2003).
[11] D. Dowek, J. F. Perez-Torres, Y. J. Picard, P. Billaud, C. Elkharrat, J. C. Houver, J. L. Sanz-Vicario, and F. Martin, Phys. Rev. Lett. **104**, 233003 (2010).
[12] V. Schmidt, Rep. Prog. Phys. **55**, 1483 (1992).
[13] M. Takahashi *et al.*, J. Electron Spectrosc. Relat. Phenom. **130**, 79 (2003).
[14] L. Nahon *et al.*, J. Chem. Phys. **125**, 114309 (2006).
[15] J. Levesque, Y. Mairesse, N. Dudovich, H. Pepin, J. C. Kieffer, P. B. Corkum, and D. M. Villeneuve, Phys. Rev. Lett. **99**, 243001 (2007).
[16] C. J. Harding *et al.*, J. Chem. Phys. **123**, 234310 (2005).
[17] T. Koide, T. Shidara, and M. Yuri, Nucl. Instrum. Methods Phys. Res. A **336**, 368 (1993).
[18] F. Schäfers *et al.*, Appl. Opt. **38**, 4074 (1999).
[19] M. Born and E. Wolf, *Principles of Optics* (Pergamon, New York, 1980).
[20] M. A. MacDonald, F. Schäfers, and A. Gaupp, Opt. Express **17**, 23290 (2009).
[21] S. Uschakow, A. Gaupp, M. A. MacDonald, and F. Schäfers, J. Phys. Conf. Ser. **425**, 152011 (2013).
[22] V. Yu. Bakman, S. V. Bobashev, and O. S. Vasyutinskii, Tech. Phys. **44**, 1103 (1999).
[23] C. J. Latimer, M. A. Macdonald, and P. Finetti, J. Electron Spectrosc. Relat. Phenom. **101–103**, 875 (1999).
[24] P. Ohresser *et al.*, J. Phys. Conf. Ser. **425**, 212007 (2013).
[25] H. Lörch, N. Scherer, T. Kerkau, and V. Schmidt, J. Phys. B **32**, L371 (1999).
[26] A. K. Kazansky, A. V. Grigorieva, and N. M. Kabachnik, Phys. Rev. Lett. **107**, 253002 (2011).
[27] W. B. Li *et al.*, J. Electron Spectrosc. Relat. Phenom. **156–158**, 30 (2007); W. B. Li, R. Montuoro, J. C. Houver, L. Journel, A. Haouas, M. Simon, R. R. Lucchese, and D. Dowek, Phys. Rev. A **75**, 052718 (2007).
[28] D. Dowek and R. R. Lucchese, *Dynamical Processes in Atomic and Molecular Physics* (Bentham, Bussum, The Netherlands, 2012), pp. 57–95.
[29] L. Nahon and C. Alcaraz, Appl. Opt. **43**, 1024 (2004).
[30] L. Nahon *et al.*, J. Synchrotron Radiat. **19**, 508 (2012).
[31] A. Lafosse, M. Lebech, J. C. Brenot, P. M. Guyon, O. Jagutzki, L. Spielberger, M. Vervloet, J. C. Houver, and D. Dowek, Phys. Rev. Lett. **84**, 5987 (2000).
[32] A. Lafosse *et al.*, J. Chem. Phys. **114**, 6605 (2001).
[33] M. Lebech, J. C. Houver, and D. Dowek, Rev. Sci. Instrum. **73**, 1866 (2002).
[34] A. Lafosse *et al.*, J. Chem. Phys. **117**, 8368 (2002).
[35] D. Dowek, M. Lebech, J. C. Houver, and R. R. Lucchese, Mol. Phys. **105**, 1757 (2007).
[36] R. R. Lucchese, A. Lafosse, J. C. Brenot, P. M. Guyon, J. C. Houver, M. Lebech, G. Raseev, and D. Dowek, Phys. Rev. A **65**, 020702 (2002).